The 14th International Topical Meeting on Nuclear Reactor Thermalhydraulics, NURETH-14
Toronto, Ontario, Canada, September 25-30, 2011

NURETH14-631

THERMALLY STRATIFIED SODIUM CHANNEL FLOW: TURBULENCE AND MODELING

M. Pellegrini[1] , H. Endo[2], H. Ninokata[1]
[1] Nuclear Engineering Department, Tokyo Institute of Technology, Japan
[2] Japan Nuclear Energy and Safety Organization (JNES), Tokyo, Japan

Abstract

Numerical simulation of sodium stratification in open channel flow has been studied with Computational Fluid Dynamics (CFD) employing an Algebraic Heat Flux Model (AHFM) closure for the turbulent heat flux. The results are validated against experimental data and the AHFM is compared with the simplified Reynolds analogy employing a constant turbulent Pr number. Influence of buoyancy on turbulence created in the mixing layer has been evaluated and its influence on the momentum and energy transport in the vertical direction assessed. It has been found that the choice of turbulent heat flux model influences the achieved results for temperature and velocity field which might affect the flow developing and persistence of stratification in the channel. Moreover both experiment and validation show the possibility of creation of a strong stratification also for low Pr number fluids, warning the stratification problem as an existing phenomenon likely to occur in liquid metal nuclear power plants.

Introduction

After the onset of Protected Loss of Flow (PLOF), due to reactor scram and pump flow-coast-down, the primary system of Liquid Metal Fast Reactors (LMFRs) experiences a drastic flow reduction (0 – 7% of the nominal conditions) and high temperature variation. The thermal transient is convected through the system as a result of decay heat removal and buoyancy forces may become significant due to the density variation and influence the transient evolution.

Previous concern about buoyancy influence on thermal stresses and pressure drops were raised and studied by Argonne National Laboratory [1]. Their experimental work, assessed with water as fluid, was set up in order to demonstrate the existence and the extent of buoyancy driven phenomena to provide useful remarks for the design of particular components (e.g. piping system, heat exchanger). However, a complete insight about the physics occurring during such transients is not discussed. In addition, while the work aims to demonstrate the stratification process in relation to the LMFRs, the justification of water employment was done through a supposed conservatism of the phenomena introduced by water compared to sodium, nevertheless it is not really understandable how to evaluate the conservatism between two different fluids. In order to clarify the processes happening during stratification the Keio University (Tokyo, Japan) performed several complete experiments about stratification in water in closed channel [2] and pipe [3-4] geometries. Their work provides interesting and important information about the mechanism occurring during such transients, the effect of gravity in the suppression of turbulence, mixing layer persistence, turbulent heat flux and counter-heat flux. However, in the work proposed in [2-4] there is no directly mention of the effects that a different Pr number would have on the assessed phenomena.

Experimental evaluation of sodium shows difficulties for the handling of the facility (e.g. high temperature, chemically reactive with air and water) and for the difficulty in the evaluation of the flow field, nevertheless a relevant amount of experimental data are available for geometry and physics of common interest (e.g. pipe, rod bundles, Rayleigh-Benard cells); however very little information is available for flow stratification in conduits.

One of the few examples of stratification experiment of a sodium flow as working fluid was performed by Mitsubishi and CRIEPI [5] in an open channel, in order to address the stratified region which can be created in the pool of a pool-type LMFR during PLOF conditions. While providing evidence about the existence of an important stratification process also in sodium turbulent flows, the above experiment does not show satisfying explanation of the effect of a higher thermal conductivity on the stratification extent and the effect of gravity on turbulence, as it was performed instead for water in more exhaustive papers [2-4].

Computational approaches therefore can overcome the above mentioned limitation providing insights and understandings of the process. The work provided by [6] in this direction shows Direct Numerical Simulation (DNS) results in channel flow for various fluids (air, water and sodium) discussing the effect of the thermal conductivity on the instability and wave formation. Even though the available results reflect some of the important issues introduced by low Pr number fluids, the mentioned work, due to the high computational costs, addresses only laminar flows which are not completely representative of stratified flows in industrial application.

Besides DNS, modelization still plays an active role in the industrial field and it is widely employed for the analysis of forced regimes, however the evaluation of buoyancy driven flows, where natural convection plays an important role on flow establishment, often shows wrong predictions of the temperature and velocity fields due to the employment of too simple modelization of the turbulent heat flux. It is considered therefore highly attractive to possess a reliable and quick computational tool (e.g. turbulence modelization for buoyancy turbulent flows) which can be demonstrated to succeed in evaluating major characteristics of buoyancy affected flows, such as during thermal stratification.

The purpose of the present work therefore is two-fold:

1. Investigation of the behavior of stratification in sodium and buoyancy effect on mixing layer;
2. Test the influence of the employment of two different approaches to model the turbulent heat flux.

1. Experimental: Domain and Spatial Discretization

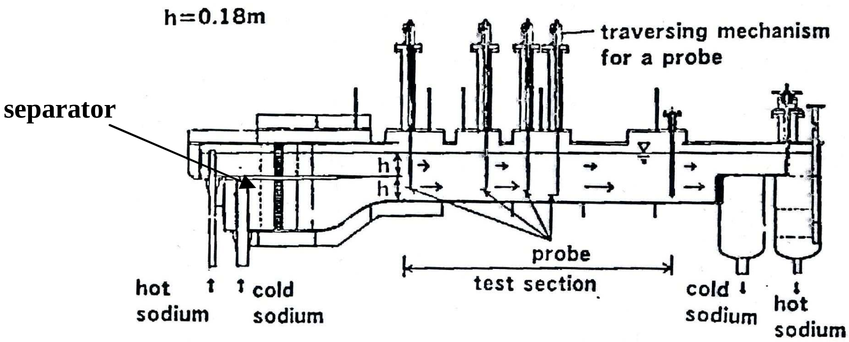

Figure 1 Experimental facility [5].

The experimental facility (Figure 1) studied in [5] consists of an open channel with a separator applied at the inlet in order to obtain two parallel flows of different velocities and temperatures. The open channel configuration was adopted to ease the acquisition of the results during the experiment [5]. Even though the present work aims to acquire knowledge for a closed geometry (e.g. pipe) the open channel flow resembles half a closed channel flow and related information can be drawn.

The two regions of the channel are of the same height (h = 0.18 m) and the discretized domain extends for x/2h = 12.5, while the provided results refer only to x/2h = 2.5. The spatial discretization is shown in Figure 2 where a boundary layer is created at the bottom wall and around the separator. Moreover, due to creation of shear layer (velocity and temperature gradients) in the middle of the domain a volumetric refiner was employed to be correctly simulate velocity and temperature gradient (measures of relevant cells are shown in Figure 2 caption). The top wall was treated with *slip* conditions in order to avoid the modelization of the interface, since not the main objective of the benchmark the evaluation of the wave formation in the open surface, which is nevertheless supposed to be small and not affecting the flow and the stratification process. The 2-dimensional domain allows to compute a high resolution of the mesh without obtaining a too heavy simulation while a fine discretization of the shear layers. The total number of cells in the grid is less than 600,000 elements.

The non dimensional numbers governing the flow are the bulk Reynolds number and the bulk Richardson number representing the ratio between buoyancy and inertial forces. The values of velocity, temperature and non dimensional numbers, adopted for the present simulation, are provided in Table 1.

Table 1 Parameters governing the benchmark.

U_1 [m/s]	U_2 [m/s]	T_h [K]	T_c [K]	ΔT [K]	Ri	Re
0.095	0.294	600.15	640.15	40	0.52	10^5

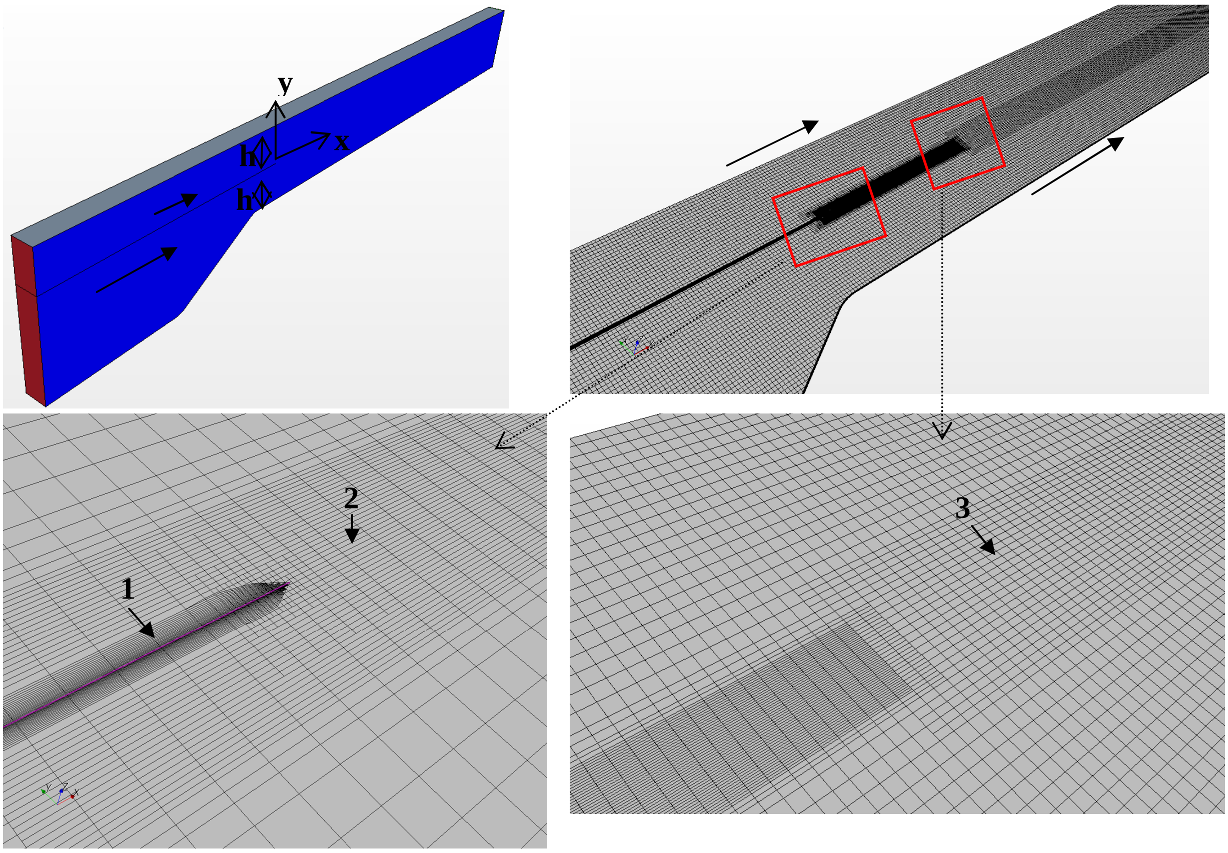

Figure 2 Geometry and 2D mesh. Solid arrows represent the flow direction. Applied dimensions: 1) boundary layer first cell, 0.1 mm; shear layer close to the wall, 1 mm, shear layer 3.75 mm.

2. Mathematical Modeling

The computational code employed in the present work is the commercial code STAR-CCM+6.02.007 [8]. The equations shown in the next chapters will be solved in second-order accuracy in space, and second order advancement in time. The convective terms are discretized with second order upwind scheme. The flow is solved as incompressible and the connection between continuity and momentum equations is achieved with Rhie-Chow pressure-velocity coupling combined with the SIMPLE algorithm. The density is assumed constant during the calculations and expression of the buoyancy force in the momentum equation follows the Boussinesq approximation (truncation to the first order of the Taylor expansion). The Unsteady RANS (URANS) equations which are employed in the analysis are :

$$\frac{\partial \langle U_j \rangle}{\partial x_j} = 0 \tag{1}$$

$$\frac{D\langle U_j\rangle}{Dt} = -\frac{1}{\rho}\frac{\partial\langle P\rangle}{\partial x_j} + \frac{\partial}{\partial x_i}\left(\nu\frac{\partial\langle U_j\rangle}{\partial x_i} - \langle\overline{u_i u_j}\rangle\right) + g\beta\left(\langle T\rangle - T_0\right)\delta_{i2} \tag{2}$$

$$\frac{D\langle T\rangle}{Dt} = \frac{\partial}{\partial x_i}\left(\frac{\kappa}{c_p\rho}\frac{\partial\langle T\rangle}{\partial x_i} - \langle\overline{\theta u_i}\rangle\right), \tag{3}$$

where the terms $\langle\overline{u_i u_j}\rangle$ and $\langle\overline{\theta u_i}\rangle$ need a closure. The study of modelization for the closure terms have struck the fluid dynamic fields since its beginning and, the more tested and reliable models can generally be found in many commercial and non commercial CFD codes. However, while many different models are implemented for the closure of the first term ($\overline{u_i u_j}$ or Reynolds stresses), e.g. *Spalart-Almaras*, *k-ε*, *k-ω* together with second and third order closure in order to take into account the anisotropy of turbulence and flow, a simple eddy-diffusivity hypothesis approach is instead generally found for the turbulent heat flux modeling. The last method consists of setting a constant value for the turbulent Prandtl number and, following the Reynolds analogy and, assuming similar behavior between the turbulent transport of momentum and heat, evaluate a turbulent eddy diffusivity. In particular indeed,

$$\overline{\theta u_i} = -\alpha_t\frac{\partial T}{\partial x_i} = -\frac{\nu_t}{\mathrm{Pr}_t}\frac{\partial T}{\partial x_i}, \tag{4}$$

where α_t is the eddy diffusivity and the turbulent Prandtl number (Pr_t) is generally set to 0.9, and this value will be adopted for the evaluation of this case further in the paper.
As shown by [9], this approach shows issues during application of flows with molecular Pr different from one (e.g. liquid metals) where temperature and velocity fields develop differently. Moreover in case, as in stratification, where velocity and temperature field are completely independent and the effect of gravity acts in only one direction, there is no connection between the turbulence features of the two fields.

2.1. Algebraic Heat Flux Model

Several are the examples of more complete models for the turbulent heat flux starting from the solution of the complete transport equation for this quantity and an additional transport equation for the temperature variance ($\overline{\theta'^2}$). However still modelization must be introduced and modeling of higher order variables represent always a complicated and not reliable task therefore, from the complete transport equation for the turbulent heat flux, a simplified solution can be achieved through the so called Algebraic Heat Flux Model (AHFM).

Accurate description of the AHFM can be found from various authors, in the present work, for the implementation and description of the model we refer to the work done in [10] by Hanjalic and Kenjeres. The modeling in STAR-CCM+ is not directly available and the one employed represents a development version for the THINS project.

The AHFM is obtained by the truncation of the parent model differential transport equations for $\overline{\theta u_i}$ [11] where the reduced expression assuming production and dissipation of k and $\overline{\theta^2}$ are locally in balance. The general algebraic expression can be written as:

$$\overline{\theta u_i} = -C^{\theta u}\frac{k}{\varepsilon}\left(C_0^{\theta u}\overline{u_i u_j}\frac{\partial T}{\partial x_j} + C_1^{\theta u}\overline{\theta u_j}\frac{\partial U_i}{\partial x_j} + C_2^{\theta u}\beta g\overline{\theta^2}\right). \tag{5}$$

Equation (5), even though simplified, contains the three major contributor from the transport equation of the turbulent heat flux, the non-uniformity of the thermal field (∇T), the mean rate of strain (∇U_i) and the attenuation or amplification of turbulence due to the effect of buoyancy $\beta g\overline{\theta^2}$. It should be noted that neglecting the effect of mean strain of rate and buoyancy leads the definition of $\overline{\theta u_i}$ to the so called generalized gradient diffusion hypothesis, where the turbulent heat flux still depends basically on the gradient of temperature but the component of the Reynolds stresses still influence its value. In case the Reynolds stress tensor its replaced with its trace the formulation of equation (5) collapses into (4) or simple gradient diffusion hypothesis (SGDH).

For the momentum flux the standard low Reynolds eddy viscosity model, $\overline{u_i u_j} = 2/3k\delta_{ij} - \nu_t\left(\partial U_i/\partial x_j + \partial U_j/\partial x_i\right)$ was employed. The eddy viscosity is defined as $\nu_t = C_\mu f_\mu k^2/\varepsilon$ where the formulation of the damping function is used according to the formulation given by [12].

The closure of the algebraic expression requires that the four scalar introduced: k, ε, $\overline{\theta^2}$, ε_θ be provided from additional transport equations, therefore finally our model will need to solve a four equation model $k-\varepsilon-\overline{\theta^2}-\varepsilon_\theta$. The equation are shown hereafter, also the transport equation for k and ε, which contain different gravity contribution respect to the terms present in case of SGDH, will be shown:

$$\frac{Dk}{Dt} = \mathsf{D}_k + P_k + P_g - \varepsilon \tag{6}$$

$$\frac{D\varepsilon}{Dt} = \mathsf{D}_\varepsilon + \frac{\varepsilon}{k}\left(C_{\varepsilon 1}P_k + P' + C_{\varepsilon 3}P_g\right) - C_{\varepsilon 2} f_2\rho\left(\varepsilon - \varepsilon_0\right) \tag{7}$$

$$\frac{D\overline{\theta^2}}{Dt} = \mathsf{D}_k + 2P_\theta - 2\varepsilon_\theta \tag{8}$$

$$\frac{D\varepsilon_\theta}{Dt} = \mathsf{D}_{\varepsilon\theta} + \frac{\varepsilon_\theta}{\overline{\theta^2}}\left(C_{\varepsilon1}^\theta P_\theta + C_{\varepsilon2}^\theta P_\theta \frac{\varepsilon}{\varepsilon_\theta}\frac{\overline{\theta^2}}{k} + C_{\varepsilon3}^\theta P_k \frac{\overline{\theta^2}}{k} + C_{\varepsilon4}^\theta \varepsilon_\theta - C_{\varepsilon5}^\theta \varepsilon \frac{\overline{\theta^2}}{k} \right) \tag{9}$$

where:

$$P_k = -\overline{u_i u_j}\frac{\partial U_i}{\partial x_j}, \quad P_g = -\beta g_i \overline{\theta u_i}, \quad P_\theta = -\overline{\theta u_i}\frac{\partial T}{\partial x_j}$$

$$P' = f_2\left(P_k + 2\mu \frac{k}{y^2} \right) \exp\left(-0.00375\,\mathrm{Re}_y^2\right)$$

$$\mathsf{D}_\varphi = \frac{\partial}{\partial x_j}\left[\left(\nu + C_\varphi f_\mu \frac{k^2}{\varepsilon} \right) \frac{\partial \varphi}{\partial x_j} \right]$$

$$f_\mu = 1 - \exp\left[-\left(C_{d0}\sqrt{\mathrm{Re}_y} + C_{d1}\,\mathrm{Re}_y + C_{d2}\,\mathrm{Re}^2 \right) \right], \quad f_2 = 1 - 0.3\exp\left(\mathrm{Re}_T^2\right), \tag{10}$$

and the index φ for D_φ, eq. (10), stands for any variables which is solved by the related transport equation.
Besides the standard coefficients employed for k and ε equations (C_k = 0.09, C_ε = 0.07, $C_{\varepsilon1} = C_{\varepsilon3}$ = 1.44, $C_{\varepsilon2}$ = 1.92). the additional coefficients are specified in Table 2.

Table 2 Adopted coefficients.

$C_0^{\theta u}$	$C_1^{\theta u}$	$C_2^{\theta u}$	$C_3^{\theta u}$	$C_{\varepsilon1}^\theta$	$C_{\varepsilon2}^\theta$	$C_{\varepsilon3}^\theta$	$C_{\varepsilon4}^\theta$	$C_{\varepsilon5}^\theta$	$\sigma_{\theta2}$	$\sigma_{\varepsilon\theta}$
0.2	0.6	0.6	0.6	1.3	0.0	0.72	2.2	0.8	1.0	1.3

3. Results

During stratification process a mixing layer is created for the interaction of two fluids with different velocity flowing in the same direction. A mixing layer is a region of the flow where velocity gradients are introduced and turbulence is generated. This process introduces additional stresses which might modify pressure losses in comparison to the one evaluated in homogeneous flows. From the theory is well known that a homogenous fluid creating a shear layer might introduce instability whit wave formation insertion at the interface, what is better known as *Kelvin-Helmholtz* instability. In the paper the discussion will refer mainly on the evaluation of those characteristics of the flow (i.e. mixing layer and instabilities) and the effect that the modelization might have on their predictions. As previously anticipated, in the analysis two modelizations of the turbulent heat flux are employed which will be referred in the rest of the paper as *AHFM* and *Const-Pr$_t$*.

3.1. Velocity Field Analysis

Iritani et al. [5] evaluated velocity profiles through electromagnetic velocimeter probes which were located at *x/2h = 2.5*, for Ri = 0.52, 0.15, 0.048.

Information on the inlet conditions are not well described in the paper therefore in the present analysis the low Ri number experiment was employed in order to compare the data with simulated isothermal conditions and to assess the turbulent intensity of the two current flows. Results in Figure 3 were achieved with a turbulence intensity of 2% showing reasonable agreement with velocity and Reynolds stresses profile. The smoother profile of velocity in the upper layer, leading to a wider shape of Reynolds stresses in Figure 3 b) is supposed to depend on the approximation of slip condition on the top wall; experimental data indeed show some influence of the open surface probably because of oscillation establishment on the same surface. Nevertheless the mixing layer prediction in the center of the domain appears substantially correct.

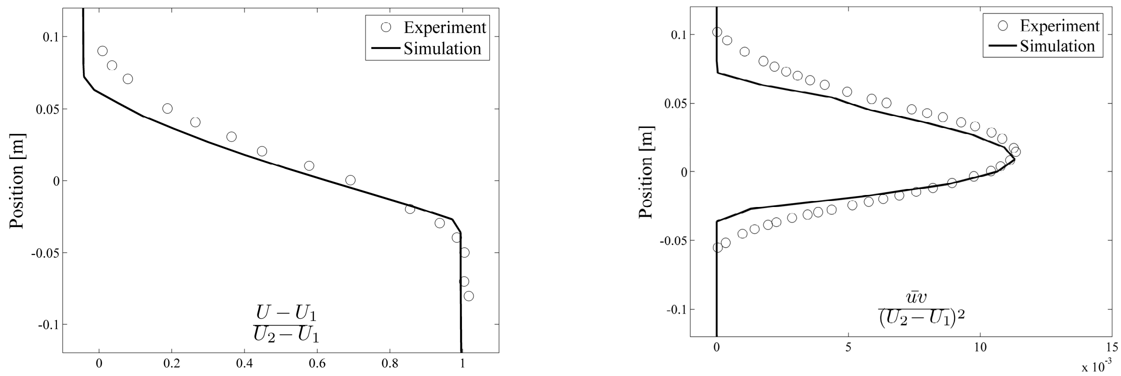

a) b)

Figure 3 Isothermal case compared with low Richardson number (Ri = 0.048) at x/2h = 2.5.

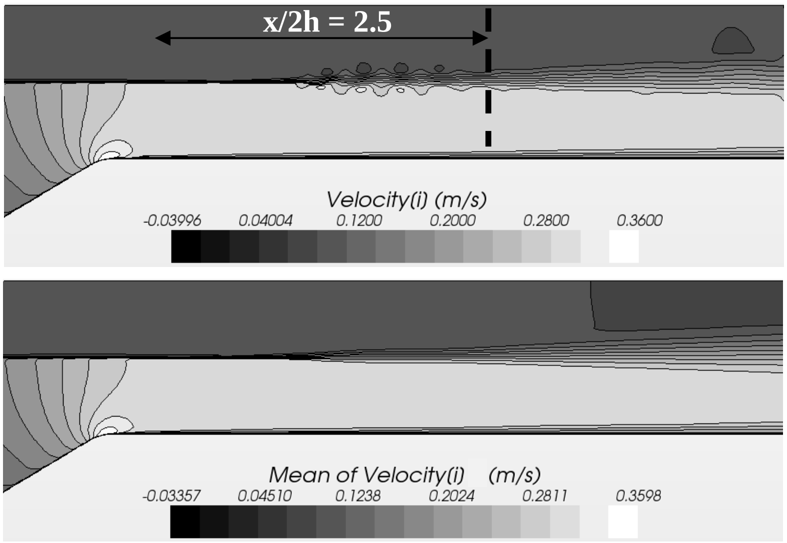

a)

b)

Figure 4 Iso-contours of instantaneous and time average velocity contours of isothermal simulation (Ri = 0).

It must be noticed that, due to high velocity difference between the two streams a Kelvin-Helmholtz instability is created and the results provided in Figure 3 are therefore time averaged. From Figure 4 indeed a wake creation exists at a certain location downstream the baffle (approximately x/2h =1 from the knife) with a similar pattern of velocity as evaluated from [13] which then attenuates further downstream. The creation of this kind of instability, as shown in the figure, increases the momentum transfer in the vertical direction. In Figure 4 b) indeed in the same location the development of the mixing layer appears growing quicker and wider for the time averaged velocity field, symbolizing the enhanced momentum transferred.
Velocity profile of the non isothermal case (see Table 1), refer to a relatively high Richardson number. The general trend of the mixing layer is described by both models and not a real difference between them can be found in the velocity prediction, at least at x/2h=2.5 from the separating wall where experimental data are available.

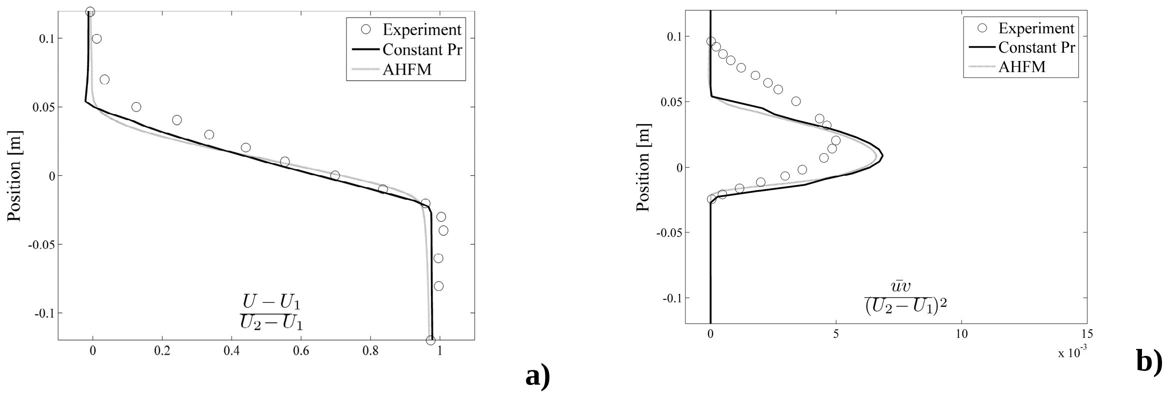

Figure 5 a) Velocity profile and b) Reynolds stresses of the non isothermal case. Results plotted at x/2h = 2.5.

In the same way also the prediction of the Reynolds stresses appears very similar between the two models and, in comparison with Figure 3 b) both can predict the suppression of the turbulence caused by the insertion of temperature difference. The suppression of turbulent stresses makes the peak of Reynolds stress components to be almost half of the isothermal case.
It is not surprising that both models can provide a similar agreement since the location we refer to is close to the separation region and therefore the velocity profile is still much influenced from the conditions imposed by the separator. From the achieved results indeed the non isothermal velocity profile is also similar to the isothermal one therefore not high influence of the temperature on the flow is assessed in this location in the time averaged analysis.
Nevertheless in Figure 6 a, b), where instantaneous iso-contours of the velocity field are shown, AHFM and const Pr_t show a different behavior. In relation to the isothermal case, the oscillation of the mixing layer predicted by AHFM appears reduced at the location close to the separator while later it amplifies. On the other hand the simpler modelization of the turbulent heat flux suppresses the oscillation introduced during the isothermal case and a steady solution is achieved even though performing a transient calculation.

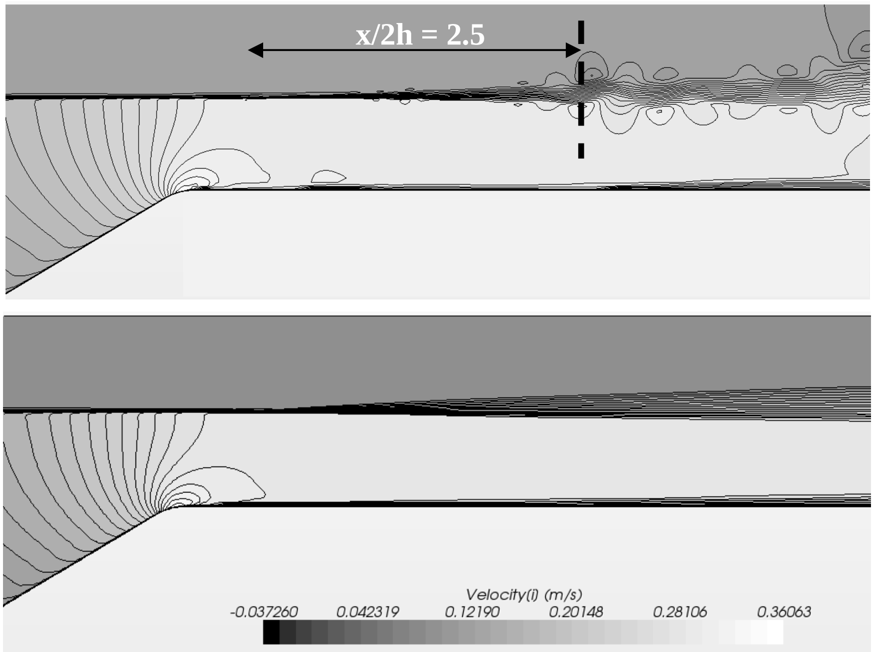

a)

b)

Figure 6 Velocity field of the non-isothermal case. a) represents the AHFM prediction, b) the const PR_t prediction.

3.1.1. Velocity integral length scale

A quantitative assessment to evaluate the mixing layer thickness is the *velocity integral length scale* (VILS). In this paper the methodology shown in [14] for its evaluation was followed, where the non-dimensional VILS is defined as:

$$\theta_u = \frac{1}{2h \cdot \Delta U^2} \int_{-h}^{h} \left(U_1 - \bar{u}(y)\right)\left(\bar{u}(y) - U_2\right) dy \,. \tag{11}$$

Figure 7 shows that the employment of *AHFM* creates a slight increase in the thickness of the mixing layer close the separator (*x/2h = 2.5*). This can be explained by the introduction of the wakes in this location in the domain; comparing Figure 4 a) and Figure 6 a) indeed this consideration appears clear. On the other side instead the constant turbulent Pr model shows a behavior similar to the isothermal case since no significant influence is predicted due to the insertion of the temperature field at location x/2h = 2.5. These results assume interest in the case of pressure drop evaluation. The additional pressure created by the mixing layer should be depending on the thickness and velocity gradient therefore, since a non negligible difference is shown between the two models, the choice of one towards the other could influence the final assessment.

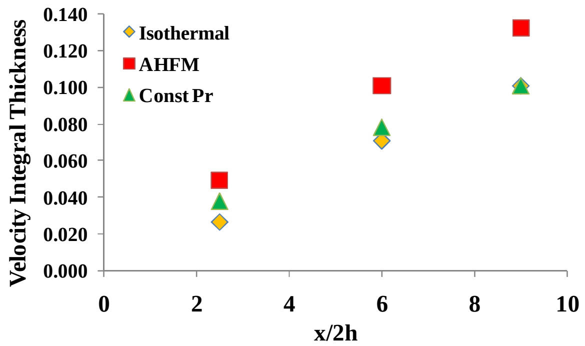

Figure 7 Velocity Integral Length Scale for Ri = 0 and Ri = 0.52 with two modelizations.

3.2. Temperature

Introduction of a temperature difference between the two currents might have a very different effect on the phenomena occurring in the simulation. Indeed a too high Richardson number should manifest in complete suppression of the instability reaching a steady solution. In Figure 8 the two models produce nevertheless very different results.

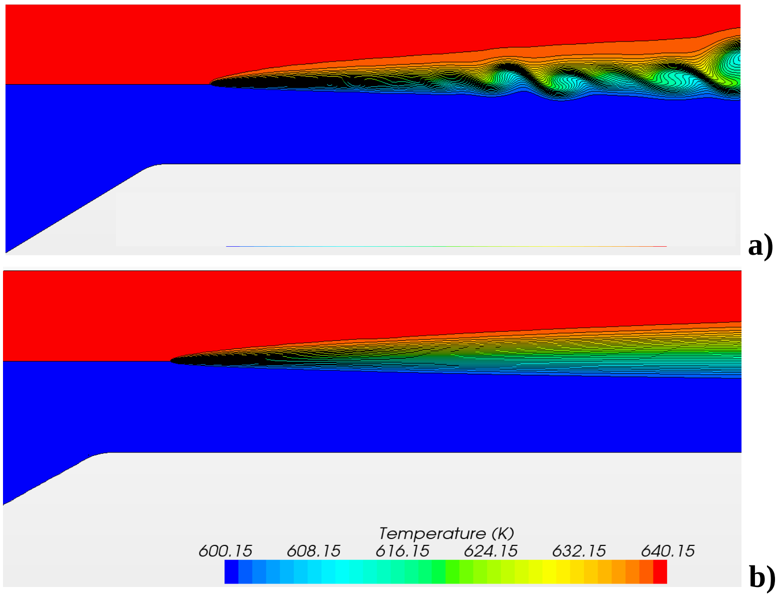

Figure 8 Contours of temperature, top on represents the instantaneous values, bottom the average. a) AHFM results, b) Const-Pr_t.

Indeed in a) the AHFM produces a very accentuated oscillation of the temperature field while, the temperature difference shows a sort of suppression of the wake creation for the simpler model. This behavior can be easily explained in relation to the results of the turbulent heat flux shown in Figure 9 b). In comparison with the experimental data indeed no model can provide correct results, nevertheless some important consideration can be traced. Const Pr_t model does show too high turbulent heat flux predictions which can be assumed to influence the creation of the oscillations; on the other hand instead AHFM underpredicts the behavior, result that can refer to the high instability predicted by the model. In this direction it has to be remembered that this analysis represents a preliminary assessment of the thermal field achieved through the AHFM and the coefficients provided in [10] are here employed (see Table 2). The referred study refers to natural convections flows, while in the present analysis forced flows with high shear and buoyancy influence is studied. Therefore a proper set of coefficients, supported by physical consideration, even though might lead to lack of generality, might help to reproduce the correct results.

Figure 9 a) moreover shows that no high difference is inserted in the temperature evaluation. This characteristic is common in fluids with low molecular Pr numbers where the molecular heat transfer represents the most important contribution. Nevertheless from these results, the models seem to give influence on the turbulent heat flux evaluation and on the developing of the thermal and momentum field in relation to the instability.

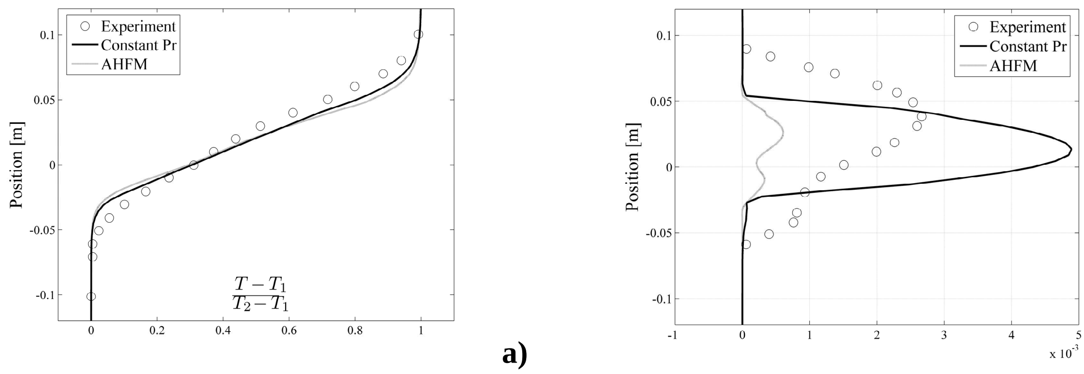

a) b)

Figure 9 Temperature a) and turbulent heat flux b) evaluated with the two models at x/2h = 2.5.

Comparison of the temperature integral length scale (TILS) (which can be derived easily from equation (11) substituting velocities with the related temperatures) shows that, while close to the separator the two models have indeed identical prediction of the temperature, further in the domain the difference increases. This high difference should not be related to the different description of the turbulent heat flux from the two models but in particular from the very different evaluation of the instabilities occurring in the thermal and velocity field. An interesting result is the decrease of the thermal thickness for sodium further in the domain predicted in location x/2h = 9, result which finds agreement with water results [3] with creation of counter-heat flux. However result further in the domain are not available and therefore comparison cannot state which one is the real or the closer behavior of the sodium flow. Nevertheless the two models introduce difference in particular for the thermal field evaluation downstream the domain and therefore further evaluation to access how much the two models can influence the prediction must be carried out.

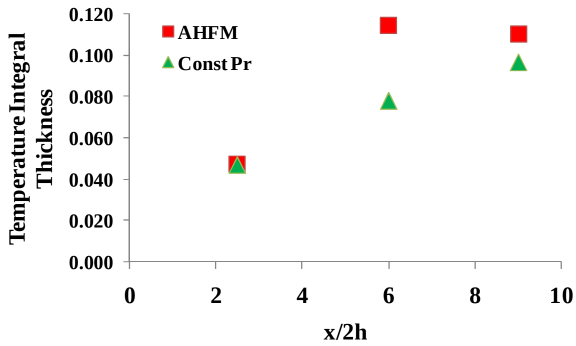

Figure 10 Temperature integral thermal thickness evaluated with the two models.

4. Conclusions

An experimental thermally stratified open channel sodium flow has been simulated as validation of URANS modeling and importance of the phenomenon for liquid metals. Comparison of AHFM with the eddy diffusivity based on the Reynolds analogy demonstrates the possibility to obtain different results for physical and turbulence values with the employment of a more complete description of the turbulent heat flux (i.e. AHFM). It was found that, even though the molecular heat transfer for sodium might have a higher influence, a different modeling of the effect of turbulence on the heat transferred, might influence the results further in the domain and final considerations about sodium behavior during transients. On the same machine with same number of processors the employment of AHFM needs 20% time longer to perform an iteration. Since the present case is two-dimensional the drawback is acceptable, nevertheless in 3D domain the calculation might slow down considerably.

In case CFD with RANS models would have been used for the evaluation of pressure drop correlations or persistence of the stratification under PLOF transients, it was shown that the evaluation of velocity and temperature mixing layers might be highly influenced by the correct choice of the turbulence model. Nevertheless the study aims also to demonstrate the possibility of a stable stratification creation in sodium flows, showing that further experimentally and computationally studies are needed in this direction for insight in sodium flow characteristics during thermal transients.

Acknowledgment

The authors would like to acknowledge the THINS project for providing the present study with the suitable tools in order to perform simulations with the AHFM and the support received during the analysis.

5. References

[1] K.E. Kasza, J.P Bobis, W.P. Lawrence, “Overview of thermal transient induced buoyancy phenomena in pipe and heat exchanger flows”, Chemical Engineering Communication, Vol. 19, 1983, pp. 295-316.

[2] Ishida, T. Ogita, K. Kobayashi, M. Maeda, “Turbulence transport phenomena across stable thermal stratified layer in a rectangular channel duct”, Transport Phenomena in Turbulent Flows Theory, Experiment and Numerical Simulation, ed. M. Hirata and N. Kasagi, pp. 335-348, Hemisphere, New York, 1988.

[3] K. Kobayashi, K. Ishida, M. Maeda, “Turbulent transport across stable thermal stratified layer in a circular pipe”, Proceeding 9th International Heat Transfer Conference, Jerusalem, Israel, Vol. 5, pp 341-346, 1990.

[4] J. Sakakibara, K. Hishida, M. Maeda, “Measurements of thermally stratified pipe flow using image-processing techniques”, Experiments in Fluids, Vol. 16, 1993, pp. 82-96.

[5] Y. Iritani, K. Nakamura, S. Ueda, A. Cho, S. Ushijima, S. Moriya, “Turbulent characteristics of thermal stratification in a sodium flow,” 4th International conference on liquid metal engineering and technology, 1988, Vol. 2 Sec. 425.1.

[6] A. B. Cortesi, G. Yadigaroglu, S. Banerjee, “Numerical investigation of the formation of the three-dimensional structures in stably stratified mixing layers”, Physics of Fluids, Vol. 10, No. 6, 1998, pp. 1449-1473.

[7] W. Rodi, “Examples of calculation methods for flow and mixing in stratified fluids”, Journal of Geophysical Research, Vol. 92, No. C5, 1987, pp. 5305-5328.

[8] STAR-CCM+6.02 User’s Guide.

[9] G. Grötzbach, “Anisotropy and buoyancy in nuclear turbulent heat transfer – critical assessment and needs for modeling”, Forchungszentrum Karlsruhe, Wissenschaftliche Brichte, FZKA 7363, December 2007.

[10] S. Kenjeres, K. Hanjalic, “Convective rolls and heat transfer in finite-length Rayleigh-Bénard convection: a two-dimensional numerical study”, Physical Review E, Vol. 62, No. 6, 2000, pp. 7987-7998.

[11] K. Hanjalic, “One-point closure models for buoyancy-driven turbulent flows”, Annual Review Fluid Mechanics, Vol. 34, 2002, pp. 321-347.

[12] F.S. Lien, W.L. Chen, M.A. Leschziner, "Low-Reynolds number eddy-viscosity modelling based on non-linear stress-strain/vorticity relations", Proc. 3rd Symp. on Engineering Turbulence Modelling and Measurements, Crete, Greece, 27-29 May, 1996.

[13] O. Tommisola, F. Lundell, P. Schlatter, A. Wherfritz, L.D. Soderberg, “Global linear and non linear stability of viscous confined plane wakes with co-flow”, Journal of Fluid Mechanics, Vol. 675, 2011, pp. 397-434.

[14] C. G. Koop, F. K. Browand, “Instability and turbulence in stratified fluid with shear”, Journal of Fluid Mechanics, Vol. 93, No. 1, 1979, pp. 135-159.